Correlated Ligand Electrons in the Transition-Metal Oxide SrRuO₃

Yuichi Seki, ¹ Yuki K. Wakabayashi ² Takahito Takeda ³, ¹ Kohdai Inagaki, ¹ Shin-ichi Fujimori ³, ³ Yukiharu Takeda, ³ Atsushi Fujimori ³, ^{3,5,6} Yoshitaka Taniyasu, ² Hideki Yamamoto ³, ² Yoshiharu Krockenberger ³, ² Masaaki Tanaka ³, ^{1,4,7} and Masaki Kobayashi ^{1,4,*}

Masaaki Tanaka[®], ^{1,4,7} and Masaki Kobayashi[®] ^{1,4,7}

Department of Electrical Engineering and Information Systems, The University of Tokyo, Bunkyo, Tokyo 113-8656, Japan

NTT Basic Research Laboratories, NTT Corporation, Atsugi, Kanagawa 243-0198, Japan

Materials Sciences Research Center, Japan Atomic Energy Agency, Sayo-gun, Hyogo 679-5148, Japan

Center for Spintronics Research Network, The University of Tokyo, 7-3-1 Hongo, Bunkyo-ku, Tokyo 113-8656, Japan

Center for Quantum Technology and Department of Physics, National Tsing Hua University, Hsinchu 30013, Taiwan

Department of Physics, The University of Tokyo, Tokyo 133-0033, Japan

Institute for Nano Quantum Information Electronics, The University of Tokyo,

4-6-1 Komaba, Meguro-ku, Tokyo 153-8505, Japan

(Received 28 November 2023; revised 20 May 2025; accepted 23 May 2025; published 25 July 2025)

In transition-metal compounds, the transition-metal d electrons play an important role in their physical properties; however, the effects of the electron correlation between the ligand p electrons have not been clear yet. In this Letter, the Ru 4d and O 2p partial density of states (PDOS) in transition-metal oxide $SrRuO_3$ involving Weyl fermions are investigated by resonant photoemission spectroscopy. The observations demonstrate that the O 2p PDOS is distorted from that predicted by first-principles calculations than the Ru 4d PDOS. The results indicate that the electron correlation in the ligand orbitals will be important to understand the electronic structure of the p-d hybridized state in strongly correlated electron systems, even with topological states.

DOI: 10.1103/n9qh-6739

Transition-metal compounds known as strongly correlated electron systems have been intensively studied due to a variety of their physical properties such as superconductivity [1], metal-insulator transition [2,3,4], and multiferroics [5,6]. The electron correlation between the transition-metal d electrons affects the electronic structure near the Fermi level $(E_{\rm F})$ and plays an important role in their physical properties [1–4,7,8]. Additionally, the interplay between electronic correlations and topological states has attracted attention as correlated topological phases for engineering the topological properties [9–15]. In high- T_c cuprate, copper oxides, and Ag₂O, photoemission studies have suggested that the values of electron correlation in O2p are about 5–6 eV [16–18]. Recently, in addition to the d electrons, the effects of the electron correlation between the ligand p electrons have been discussed theoretically and experimentally in transition-metal compounds; electroncorrelation in O 2p orbitals varying in different families in cuprates [19], observation of the delocalized ligand Ge/Te p orbitals in van der Waals magnet FeGeTe [20], spinpolarized electronic state on the ligand N 2p orbital in GaN:Eu [21]. However, it has not been clear yet how the ligand electron correlation affects the physical properties of transition-metal compounds.

Transition-metal oxide SrRuO₃ (SRO), which crystallizes in a pseudocubic perovskite structure as shown in Fig. 1(a), has been intensively investigated for more than 60 years due to its unique physical properties such as metallic transport and perpendicular magnetic anisotropy [3,22-28]. In this Letter, SRO is a model system for clarifying the relationship between the electronic state of the ligand O2p and its macroscopic physical properties since the recent improvement of the crystallinity in the thin films allowed us to access the intrinsic electronic structure of the coherent Ru 4d-O 2p hybridized states [29–32]. Indeed, thanks to the ultrahigh crystal quality, the quantum transport phenomena of Weyl fermions in ultrahigh-quality thin films have recently been observed [33–38]. In addition to the quantum transport measurements [35,39], combinations of first-principles calculations with other experiments such as neutron scattering [40] and angle-resolved photoemission spectroscopy [41] for SRO suggest the existence of the Weyl nodes in the electronic structure near $E_{\rm F}$. Figure 1(b) illustrates the crystal-field splitting and the spin configuration of the Ru 4d orbitals. Because of the octahedral (O_h) crystal field formed by the ligand O ions, the degenerate Ru 4d orbitals are split into e_q and t_{2q} orbitals with the low-spin configuration $(t_{2q\uparrow}^3, t_{2q\downarrow}^{-1})$ [3,42].

In this Letter, we have elucidated the effect of the correlated ligand electrons by direct observations of the $Ru\,4d$ and $O\,2p$ partial density of states (PDOS) in 4d

^{*}Contact author: masaki.kobayashi@ee.t.u-tokyo.ac.jp

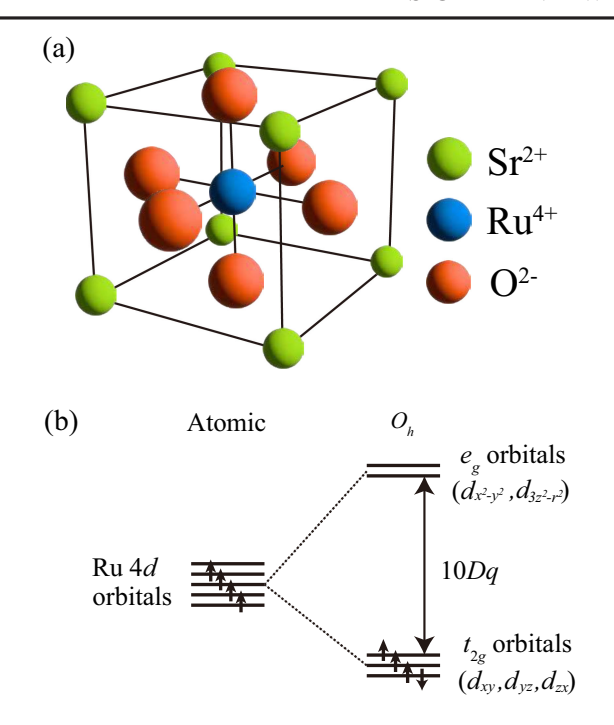


FIG. 1. Schematic view of the perovskite oxide $SrRuO_3$. (a) Perovskite crystal structure of SRO. (b) Electron and spin configurations in the degenerate $Ru\,4d$ orbitals in an isolated Ru atom and their separation due to the octahedral crystal field (O_h) in SRO. Here, 10Dq is the crystal-field splitting. A black arrow on the energy levels represents an electron with a spin.

transition-metal oxide SRO using resonant photoemission spectroscopy (RPES). Here, there have been few reports of the O K RPES on transition-metal oxides [18,43,44] because the resonant photoemission process is principally ineffective for the nearly closed shell configuration of the ligand element, especially for O with high electronegativity. The experimental results demonstrate that the Ru 4d PDOS is significantly different from the O2p PDOS in the p-dhybridized state near E_F , which is against the general belief that the feature of p PDOS is similar to that of d PDOS due to the p-d hybridization, as predicted by first-principles calculations [45,46]. The electron-electron Coulomb energy between the ligand O2p electrons (U_{pp}) estimated experimentally is much larger than that between the Ru4d electrons (U_{dd}) in SRO. The resonant enhancement of the O2p PDOS at the strong Ru4d-O2p XAS peak due to the ultrahigh crystal quality of the film allows us to evaluate the effect of U_{pp} in a transition-metal oxide quantitatively for the first time. Based on the findings, we discuss the role of the correlated ligand O2p for the emergence of the Weyl fermions in SRO. This provides experimental evidence that the electron correlation between the p electrons makes the PDOS of the metal-d and ligand-porbitals significantly different near $E_{\rm F}$.

An ultrahigh-quality SRO film with its thickness of 60 nm was grown on a SrTiO₃ (STO) (001) substrate by a custom-designed molecular beam epitaxy (MBE) setup

equipped with multiple e-beam evaporators of Sr and Ru. Here, the growth parameters were optimized by Bayesian optimization, which is a machine learning technique for parameter optimization [34,35], resulting in the fabrication of an ultrahigh-quality SRO thin film with residual resistivity ratio RRR = 56. Generally, the purity and crystalline quality of metallic electronic systems are evaluated by RRR and large RRR values are required to observe quantum transport phenomena [35,47]. The compressive strain on the SRO layer from the STO substrate was about 0.6% [33] (see Supplemental Material I for the crystal structure [48]). Soft x-ray absorption spectroscopy (XAS) and photoemission spectroscopy (PES) measurements were performed at the undulator beamline BL23SU of SPring-8. The monochromator energy resolution $E/\Delta E$ was about 10 000 and the beam spot size was $< 200 \mu m$ in diameter. The PES measurements were conducted with an SES-2002 electron analyzer (Gammadata-Scienta Co.Ltd.) at 28 K at a base pressure of 1.7×10^{-8} Pa. The XAS spectra were taken in the total-electron yield (TEY) mode. In the PES measurements, the overall energy resolutions including the thermal broadening were 103 and 110 meV for the incident photon energies ($h\nu$) of 526 and 529 eV, and 115 and 135 meV for 454 and 463 eV with narrower slit width, respectively. The position of $E_{\rm F}$ was calibrated by measuring evaporated Au in electrical contact with the

To elucidate the Ru 4d states in SRO, we have conducted the XAS and RPES at the Ru M edge. Figure 2(a) shows the Ru $M_{2,3}$ -edge XAS spectrum of the SRO film. The line shape of the Ru $M_{2,3}$ spectrum well coincides with previous reports on ultrahigh-quality SRO films [30,31]. Additionally, the core-level spectrum is comparable to the electronic structure determined earlier (see Fig. S1 in Supplemental Material [48]). The energy positions of M_3 ($h\nu \sim 463$ eV) and M_2 ($h\nu \sim 486$ eV) absorption peaks correspond to the transitions from Ru $3p_{3/2}$ and Ru $3p_{1/2}$ core levels into the unoccupied Ru 4d states, respectively [49].

As shown in Fig. 2(b), the Ru M_3 on- and off-resonance PES spectra are taken at $h\nu = 463$ and 454 eV, respectively [indicated in Fig. 2(a)]. The spectral line shapes demonstrate an intense peak structure derived from the coherent quasiparticle states near $E_{\rm F}$, which is one of the characteristic features of high-quality SRO thin films [30,31,50]. The intensity of the Ru 4d coherent quasiparticle state is enhanced at $h\nu = 463$ eV on resonance. As shown in the lower part of Fig. 2(b), the Ru 4d PDOS has been obtained as the difference between the on- and off-resonant spectra. The sharp peak in the spectrum reflects the coherent states near $E_{\rm F}$. With the increase of RRR value, the coherent quasiparticle peak becomes more intense [50] and, therefore, the observation of the prominent coherent peak reflects the high crystallinity of the measured film. Considering the reports from several theoretical and experimental studies [30,31,45,51,52], the coherent states observed near $E_{\rm F}$

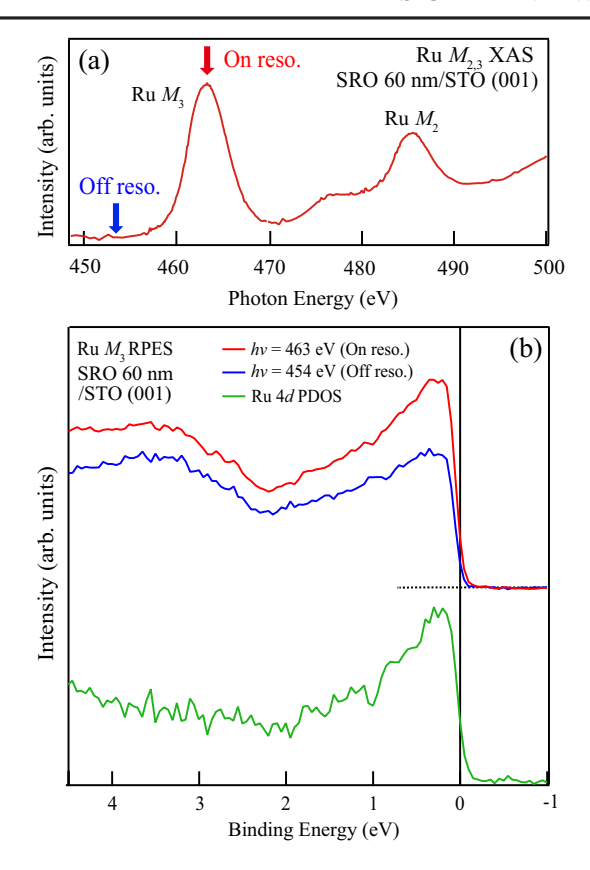


FIG. 2. Ru $M_{2,3}$ XAS and M_3 PES spectra of an ultrahigh-quality SrRuO₃/SrTiO₃ thin film. (a) Ru $M_{2,3}$ XAS spectrum. Red and blue arrows show the photon energies at which on- and off-resonance spectra were taken. (b) Ru M_3 RPES spectra. The on- and off-resonant spectra have been measured at $h\nu=463$ and 454 eV, respectively. The Ru 4d PDOS is obtained as the difference between the on- and off-resonance spectra.

probably correspond to the Ru 4d t_{2g} -O 2p antibonding states (t_{2g}^{a}). The existence of the coherent states in the Ru 4d PDOS indicates that the Ru 4d electrons predominantly contribute to the transport properties of SRO.

In addition to the Ru 4d states, the O 2p states in the valence-band structure near $E_{\rm F}$ have been analyzed using XAS and RPES at the O K edge. Figure 3(a) shows the O K-edge XAS spectrum around the energy region corresponding to the absorption into the unoccupied Ru 4d-O 2p hybridized states. From the similarity of the spectral line shapes between the present and the previous XAS spectra on ultrahigh-quality SRO films [30,31], the absorption peak at 529 eV is assigned to transitions into t_{2q}^{a} and the structures in the energy range of 530-534.5 eV are ascribed to transitions into Ru $4d e_q$ -O 2p hybridized states. The intensity of the Ru 4d t_{2q} absorption peak is higher and sharper than that of the Ru $4d e_q$ components determined in previous studies [51,53-57], reflecting the long lifetime of quasiparticles in the $t_{2g}^{\ a}$ orbital near $E_{\rm F}$. This is consistent with the previous studies on ultrahigh quality SRO thin films [30,32,34], providing us with further evidence for the

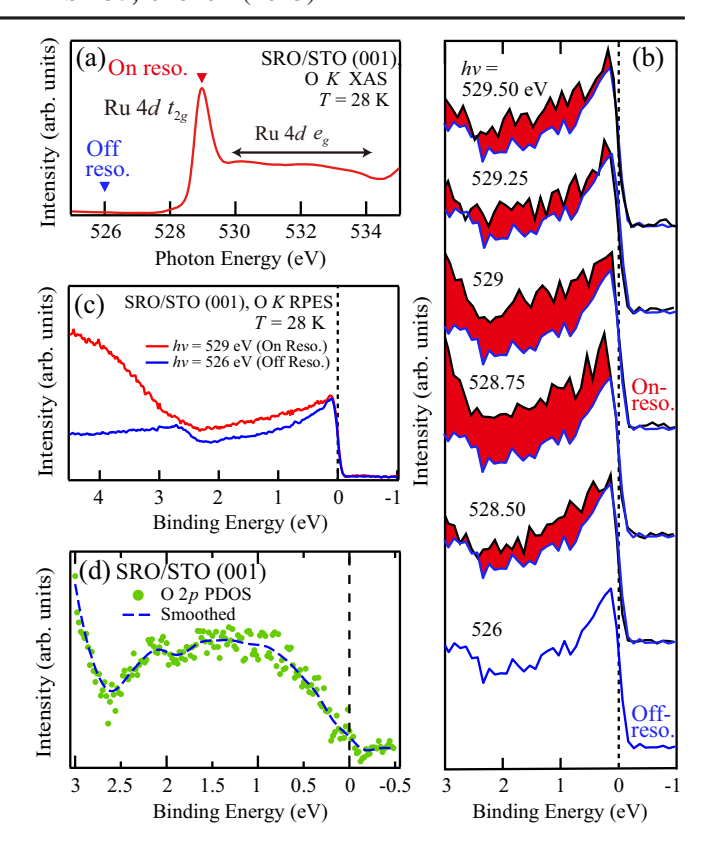


FIG. 3. O K XAS and RPES spectra of an ultrahigh-quality $SrRuO_3/SrTiO_3$ thin film. (a) O K-edge XAS spectrum. (b) Series of RPES spectra of the valence band. The spectra are taken at photon energies indicated as downward triangles in (a) ($h\nu=526-529.50$ eV. The red areas are positive differences relative to the off-resonance spectrum. (c) Comparison between the on- $(h\nu=529$ eV) and off-resonance ($h\nu=526$ eV) valence-band PES spectra. (d) O 2p PDOS obtained as the difference between the on- and off-resonant valence-band spectra. The smoothed line for the data of the O 2p PDOS is also shown.

high crystallinity of the measured sample. Figure 3(b) shows the O K RPES spectra near $E_{\rm F}$ taken with varying incident photon energies in the O K XAS region. In comparison of the RPES spectra with the off-resonance spectrum $(h\nu = 526 \text{ eV})$, the resonant enhancement is maximized approximately at $h\nu = 529$ eV. The $h\nu$ dependence of the PES intensity suggests the on-resonance energy is $h\nu = 529$ eV. Since the resonant enhancement in PES (Super Coster-Kronig transition) requires hole states in the valence band of the objective element, this result indicates that the ligand O2p band has a finite number of holes [58,59]. As this enhancement occurs in parallel with the electron excitation into the unoccupied states in t_{2q}^{a} orbitals, the existence of the hole states suggests a portion of O2porbitals becomes unoccupied and composes part of the holes in the t_{2g}^{a} orbitals. Figure 3(c) shows the O K on- and offresonance PES spectra taken at $h\nu = 529$ and 526 eV, respectively. On-resonance spectrum has two enhanced features, one at $E_B \ge 2.7\,$ eV and the other at $0 \le E_B \le 2.5\,$ eV. The former is ascribed to the excitation from the O2p nonbonding band [49,51,55] and a peripheral part of O(KLL) Auger emission [19,44,57,60,61] in which the peak position shifts with $h\nu$ [see Fig. S4(a) in Supplemental Material [48]]. Figure 3(d) shows the O2p PDOS as the difference between the on- and off-resonance spectra, where the contribution of the second order light has been removed (see Sec. III in Supplemental Material [48]). It should be noted here that the O2p PDOS in the t_{2g}^{a} band lies between $0 \le E_B \le 2.5$ eV. Compared with the Ru 4d PDOS shown in Fig. 2(b), the O2p PDOS shows a relatively broader peak centered around $E_B = 1.5$ eV with a finite but low intensity at E_F .

In the RPES measurements, the Ru 4d PDOS [Fig. 2(b)] and the O 2p PDOS [Fig. 3(d)] in t_{2g}^{a} band near $E_{\rm F}$ have been observed. Based on our experimental findings, the electronic structure of SRO realized by the Ru $4d t_{2q}$ -O 2phybridization is schematically illustrated in Fig. 4(a). From the different spectral shapes of the Ru 4d and O 2p PDOSs, it is probable that the Ru 4d and the O 2p PDOSs unequally contribute to the t_{2q}^{a} bands as indicated in Fig. 4(a): The $Ru\,4d$ PDOS has coherent states near the $E_{\rm F}$ leading to the itinerant nature. In contrast, the O2p PDOS gradually diminishes toward $E_{\rm F}$ and demonstrate small DOS near the $E_{\rm F}$. That is pseudogap behavior observed in strongly correlated electron systems [3,4]. The nonbonding and the bonding bands $(t_{2g}^{\ b})$ are also observed in the valence-band PES spectra [see Fig. S3(b) in Supplemental Material [48]]. Considering the excitation energy for the O K RPES corresponding to the peak of the x-ray magnetic circular dichroism spectrum [30] and the probing depth that possibly observes the coherent peak in the Ru 4d PDOS, it is likely that the obtained O2p PDOS reflects the bulk property of SRO, not surface contamination (see details in Sec. IV in Supplemental Material [48]).

Here we discuss the possible scenario for the difference in the observed Ru 4d and O2p PDOS spectra. The pseudogap structure of the O2p PDOS can be explained by the effect of electron correlations, as is the case for Mott-Hubbard-type insulators [2]. In detail, O2p-derived t_{2g}^a electrons are affected by relatively strong electron correlations compared to the Ru 4d-derived t_{2g}^a electrons, as discussed below. Considering the p-d hybridization, the wave function Ψ of the ground states for the RuO $_6$ cluster in SRO is given by

$$\Psi = C_0 |d^4\rangle + C_1 |d^5\underline{L}\rangle + C_2 |d^6\underline{L^2}\rangle + \dots, \tag{1}$$

where \underline{L} denotes a hole in the O 2p ligand band and $C_i(i=0,1,2,...)$ is the linear combination coefficients. $|d^{n+i}\underline{L}^i\rangle$ configurations are realized by charge transfer from the O 2p to Ru 4d bands via strong hybridization. Since the charge-transfer states involve states with a finite number of holes in the O 2p band, the influence of electron correlation on such states with holes in the O 2p band is expected to be

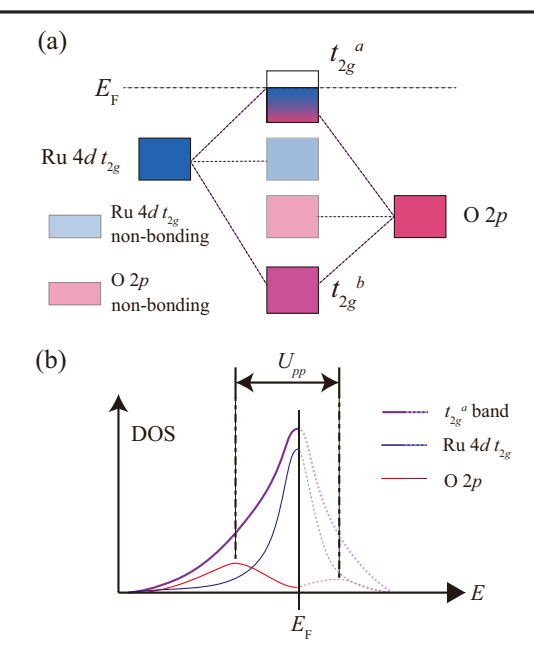


FIG. 4. Band diagram of $SrRuO_3$. (a) Schematic energy diagram of the valence-band structure through the $Ru\ 4d$ - $O\ 2p$ hybridization in SRO. " t_{2g}^{a} " and " t_{2g}^{b} " indicate the antibonding and bonding bands, respectively. The gradation in the t_{2g}^{a} band describes the transition of the dominant components of the $Ru\ 4d$ and $O\ 2p$ electrons, i.e., the orbital-dependent distributions of $Ru\ 4d$ and $O\ 2p$ PDOSs. (b) Schematic picture of the $Ru\ 4d$ and $O\ 2p$ PDOS in t_{2g}^{a} band near E_F . The DOS is drawn with a solid line below E_F and dotted line above E_F . The U_{pp} indicates the on-site Coulomb energy for electrons in the $O\ 2p$ band.

finite for the states near E_F , whereas the O2p electron correlation in the $|d^4\rangle$ state with fully occupied O 2p band is ineffective [62]. Considering the mixture of the terms in Eq. (1) (called as configuration interaction), the O 2p PDOS in the t_{2a}^{a} band is caused by the cross terms with the chargetransfer states. Hence, it is expected that the angular-orbital (p or d) dependent distributions of the PDOS originate from the presence or absence of the charge-transfer states. Furthermore, the electron correlations of the O2p likely affect the distribution of the PDOS in the t_{2q}^{a} band. To verify this hypothesis, the on-site Coulomb energy of the O2pelectrons U_{pp} is estimated as $U_{pp} = 5.7 \pm 0.1$ eV using the Cini-Sawatzky method [see Fig. S4(c) in Supplemental Material [48]] and found to be significantly larger than that of Ru 4d $U_{dd} = 1.7-3.1$ eV [63-65]. Based on this relationship and the multiple configurations in Ψ , t_{2q}^{a} band can be schematically described as shown in Fig. 4(b). In contrast to coherent Ru 4d PDOS, the larger U_{pp} causes the pseudogap structure in the O 2p PDOS (cross terms with the charge-transfer states in $|\Psi|^2$). It follows from these arguments that the difference between the Ru 4d and O 2p PDOS in t_{2a}^{a} band comes from the different electron correlations depending on the elemental orbital characters.

Based on our observation, we can further discuss the physical properties of SRO. The pseudogap behavior of the O2p PDOS near E_F indicates that the O2p state hardly contributes to the transport properties of SRO and the high itineracy of the quasiparticle around $E_{\rm F}$ predominantly comes from the Ru4d state [30]. As for the quantum transport phenomena of SRO, the emergence of the Weyl fermion in the p-d hybridized state is related to the balance between the Coulomb interaction and the band width [9,10]. Generally, topological states with linear band dispersion are weakly correlated because of the relatively large band widths compared with the Coulomb interactions. Considering the strong U_{pp} of the O2p PDOS, it is possible that the hybridization with the O2p negatively acts for the emergence of the Weyl fermion. However, in the energy range near $E_{\rm F}$ that the Weyl nodes exist, the O 2p PDOS with the pseudogap behavior less contributes to the transport property than the Ru 4d PDOS, Thus, the emergence of the Weyl nodes mainly originates from the inherent characteristics of the Ru 4d PDOS even in the p-d hybridized state and the hybridization with O2p may contribute to extend the band width of the hybridized state.

Additionally, the presence of the charge-transfer states $|d^{n+i}\underline{L}^i\rangle$ can also explain the nontrivial finite magnetic moment on the ligand O ions observed by x-ray magnetic circular dichroism [30,31]. Since Ru in the SRO (001) has spin-polarized 4d electrons [22,42], the ligand electrons with minority spins tend to be involved in the charge-transfer states from the fully occupied O 2p orbitals. It is probable that this spin-selective charge transfer from the O 2p band induces spin polarization in the O 2p band, which explains the nontrivial magnetic moment on the ligand O ions in SRO.

Traditionally, it has been considered that electron correlation between d electrons U_{dd} plays an important role in the physical properties of strongly correlated electron systems. Indeed, in previous theoretical studies for transition-metal compounds, only U_{dd} is considered for electron correlation, leading to basically similar distributions of PDOS irrespective of the orbital characteristics (p or d) in the p-d hybridized states [34,37,38,44,52,64,65]. As discussed above, the present observations demonstrate that the spectral line shape of the d PDOS is dramatically different from that of the p PDOS in the p-d hybridized states because of the large Coulomb energy of the ligand p states U_{pp} compared to that of the transition-metal d states U_{dd} . This consequence raises a question about the conventional description of transition metal d-ligand p orbital hybridization, that is, the uniform mixture of d and p electrons in the hybridized states, in particular, in 4d and 5d transitionmetal oxides, where U_{dd} is relatively small. This consideration will be generally applied to understanding the electronic structures of ligand elements in correlated p-d hybridized systems [19,20,66,67]. The results suggest that further intensive theoretical and experimental studies on the electronic structure caused by ligand hybridization will extend our understanding of physical backgrounds effective in the fascinating properties of the correlated ligand materials.

In conclusion, we have performed XAS and RPES measurements on an ultrahigh quality SRO thin film to elucidate the ligand electron correlation. The observations demonstrate that the Ru 4d PDOS shows a different spectral line shape from the O 2p PDOS even in their hybridized states in the vicinity of E_F : The Ru 4d PDOS establishes an intense coherent peak across $E_{\rm F}$ and, therefore, predominantly contributes to the itinerant electronic behavior, whereas the O2p PDOS turns out to show a pseudogaplike spectral line shape in the vicinity of $E_{\rm F}$. This result is different from theoretical calculations showing the relatively uniform distributions of the PDOSs in the hybridized state, where the p electrons are assumed to have negligible electron correlation compared to the d orbitals. Based on our experimental findings, the dramatically different d and p PDOSs in the p-d hybridized state are explained by the charge transfer from the Ru $4d t_{2q}$ orbital to the O 2p orbital and the electron correlation of the ligand O2p orbitals which is stronger than that of the Ru 4d orbitals. Actually, the value of U_{pp} estimated by the Cini-Sawatzky method is double of U_{dd} predicted from theoretical calculations. It is likely that the nontrivial finite magnetic moment on the ligand O²⁻ ions originates from the spin-selective charge transfer from the O2p band to the spin-polarized Ru 4d band. As for the quantum transport property of SRO, the O2p PDOS with pseudogap behavior less contributes to the transport property due to the relatively strong U_{pp} and the emergence of the Weyl fermion probably originates from the inherent characteristics of the Ru 4d PDOS in the p-d hybridized state.

The present results suggest a general perspective that the transition-metal d and ligand p PDOSs in the p-d hybridized states possibly depend on their orbital characteristics in transition-metal compounds. This provides experimental evidence that the electron correlation between the p electrons makes PDOS of the metal-d and ligand-p orbitals significantly different near $E_{\rm F}$. Based on the present findings, the electron correlation in the ligand orbital, especially for ligand elements with high electron negativity such as O and N, will play an important role in understanding the electronic structure of the p-d hybridized states in strongly correlated electron systems.

Acknowledgments—The authors are grateful to H. Katayama-Yoshida for informative discussion. This work was supported by Grants-in-Aid for Scientific Research Grants-in-Aid for Scientific Research (19K21961, 20H05650, 22H04948, and 22K03535), CREST program (JPMJCR1777) of Japan Science and Technology Agency. This work was partially supported by the Spintronics Research Network of Japan (Spin-RNJ). This work was

carried out under the Shared Use Program of Japan Atomic Energy Agency (JAEA) Facilities (Proposal No. 2022A-E23) supported by JAEA Advanced Characterization Nanotechnology Platform as a program of "Nanotechnology Platform" of the Ministry of Education, Culture, Sports, Science and Technology (MEXT) (Proposals No. JPMXP1222AE0031). The experiment at SPring-8 was accepted by the Japan Synchrotron Radiation Research Institute (JASRI) Proposal Review Committee (Proposal No. 2020A3841). A. F. acknowledges the support from the National Science and Technology Council of Taiwan (Grant No. 113-2112-M-007-033), and the Yushan Fellow Program from the Ministry of Education of Taiwan.

Y. S. and M. K. conceived the idea and designed the experiments. Y. S., Y. K. W., and M. K. planned the synchrotron experiments. Y. K. W., Y. Taniyasu, H. Y., and Y. K. grew the sample. Y. K. W. performed the sample characterizations. Y. S., T. T., K. I., M. K., S.-I. F., and Y. Takeda carried out the XAS and PES measurements. Y. S. and M. K. analyzed and interpreted the data supported by input from A. F. and M. T., Y. S. and M. K. wrote the Letter supported by input from all authors.

- [1] P. W. Anderson, Science 235, 1196 (1987).
- [2] M. Imada, A. Fujimori, and Y. Tokura, Rev. Mod. Phys. 70, 1039 (1998).
- [3] G. Koster, L. Klein, W. Siemons, G. Rijnders, J. S. Dodge, C. B. Eom, D. H. A. Blank, and M. R. Beasley, Rev. Mod. Phys. 84, 253 (2012).
- [4] K. Yoshimatsu, T. Okabe, H. Kumigashira, S. Okamoto, S. Aizaki, A. Fujimori, and M. Oshima, Phys. Rev. Lett. 104, 147601 (2010).
- [5] C. A. F. Vaz, J. Phys. Condens. Matter 24, 333201 (2012).
- [6] W. Prellier, M. P. Singh, and P. Murugavel, J. Phys. Condens. Matter 17, R803 (2005).
- [7] A. Urushibara, Y. Moritomo, T. Arima, A. Asamitsu, G. Kido, and Y. Tokura, Phys. Rev. B 51, 14103 (1995).
- [8] S. Satpathy, Z. S. Popovic, and F. R. Vukajlovic, Phys. Rev. Lett. **76**, 960 (1996).
- [9] D. Pesin and L. Balents, Nat. Phys. 6, 376 (2010).
- [10] W. Witczak-Krempa, G. Chen, Y. B. Kim, and L. Balents, Annu. Rev. Condens. Matter Phys. 5, 57 (2014).
- [11] K. Kuroda et al., Nat. Mater. 16, 1090 (2017).
- [12] W. Qin, L. Li, and Z. Zhang, Nat. Phys. 15, 796 (2019).
- [13] Y. Shao, A. N. Rudenko, J. Hu, Z. Sun, Y. Zhu, S. Moon, A. J. Millis, S. Yuan, A. I. Lichtenstein, D. Smirnov, Z. Q. Mao, M. I. Katsnelson, and D. N. Basov, Nat. Phys. 16, 636 (2020).
- [14] Y. Xu, J. Zhao, C. Yi, Q. Wang, Q. Yin, Y. Wang, X. Hu, L. Wang, E. Liu, G. Xu, L. Lu, A. A. Soluyanov, H. Lei, Y. Shi, J. Luo, and Z.-G. Chen, Nat. Commun. 11, 3985 (2020).
- [15] Y. Li, T. Oh, J. Son, J. Song, M. K. Kim, D. Song, S. Kim, S. H. Chang, C. Kim, B.-J. Yang, and T. W. Noh, Adv. Mater. 33, 2008528 (2021).

- [16] J. Ghijsen, L. H. Tjeng, J. van Elp, H. Eskes, J. Westerink, and G. A. Sawatzky, Phys. Rev. B 38, 11322 (1988).
- [17] L. H. Tjeng, M. B. J. Meinders, J. van Elp, J. Ghijsen, and G. A. Sawatzky, and R. L. Johnson, Phys. Rev. B 41, 3190 (1990).
- [18] L. H. Tjeng, C. T. Chen, and S.-W. Cheong, Phys. Rev. B 45, 8205 (1992).
- [19] A. Chainani et al., Phys. Rev. B 107, 195152 (2023).
- [20] K. Yamagami, Y. Fujisawa, B. Driesen, C. H. Hsu, K. Kawaguchi, H. Tanaka, T. Kondo, Y. Zhang, H. Wadati, K. Araki, T. Takeda, Y. Takeda, T. Muro, F. C. Chuang, Y. Niimi, K. Kuroda, M. Kobayashi, and Y. Okada, Phys. Rev. B 103, L060403 (2021).
- [21] A. Masago, H. Shinya, T. Fukushima, K. Sato, and H. Katayama-Yoshida, AIP Adv. 10, 025216 (2020).
- [22] J. J. Randall and R. Ward, J. Am. Chem. Soc., 81, 2629 (1959).
- [23] J. Okamoto, T. Mizokawa, A. Fujimori, I. Hase, M. Nohara, H. Takagi, Y. Takeda, and M. Takano, Phys. Rev. B 60, 2281 (1999).
- [24] P. B. Allen, H. Berger, O. Chauvet, L. Forro, T. Jarlborg, A. Junod, B. Revaz, and G. Santi, Phys. Rev. B 53, 4393 (1996).
- [25] L. Klein, J. S. Dodge, T. H. Geballe, A. Kapitulnik, A. F. Marshall, L. Antognazza, and K. Char, Appl. Phys. Lett. 66, 2427 (1995).
- [26] M. Izumi, K. Nakazawa, Y. Bando, Y. Yoneda, and H. Terauchi, J. Phys. Soc. Jpn. 66, 3893 (1997).
- [27] A. P. Mackenzie, J. W. Reiner, A. W. Tyler, L. M. Galvin, S. R. Julian, M. R. Beasley, T. H. Geballe, and A. Kapitulnik, Phys. Rev. B **58**, R13318 (1998).
- [28] L. Klein, J. S. Dodge, C. H. Ahn, G. J. Snyder, T. H. Geballe, M. R. Beasley, and A. Kapitulnik, Phys. Rev. Lett. 77, 2774 (1996).
- [29] S. Kunkemöller, K. Jenni, D. Gorkov, A. Stunault, S. Streltsov, and M. Braden, Phys. Rev. B 100, 054413 (2019).
- [30] Y. K. Wakabayashi, M. Kobayashi, Y. Takeda, K. Takiguchi, H. Irie, S.-I. Fujimori, T. Takeda, R. Okano, Y. Krockenberger, Y. Taniyasu, and H. Yamamoto, Phys. Rev. Mater. 5, 124403 (2021).
- [31] Y. K. Wakabayashi, M. Kobayashi, Y. Takeda, M. Kitamura, T. Takeda, R. Okano, Y. Krockenberger, Y. Taniyasu, and H. Yamamoto, Phys. Rev. Mater. 6, 094402 (2022).
- [32] Y. K. Wakabayashi, M. Kobayashi, Y. Seki, Y. Kotani, T. Ohkouchi, K. Yamagami, M. Kitamura, Y. Taniyasu, Y. Krockenberger, and H. Yamamoto, APL Mater. 12, 041119 (2024).
- [33] Y. K. Wakabayashi, T. Otsuka, Y. Krockenberger, H. Sawada, Y. Taniyasu, and H. Yamamoto, APL Mater. 7, 101114 (2019).
- [34] Y. K. Wakabayashi, T. Otsuka, Y. Taniyasu, H. Yamamoto, and H. Sawada, Appl. Phys. Express 11, 112401 (2018).
- [35] K. Takiguchi, Y. K. Wakabayashi, H. Irie, Y. Krockenberger, T. Otsuka, H. Sawada, Masaaki Tanaka, Yoshitaka Taniyasu, and Hideki Yamamoto, Nat. Commun. 11, 4969 (2020).
- [36] Y. K. Wakabayashi, S. Kaneta-Takada, Y. Krockenberger, K. Takiguchi, S. Ohya, M. Tanaka, Y. Taniyasu, and H. Yamamoto, AIP Adv. 11, 035226 (2021).
- [37] S. Kaneda-Takada, Y. K. Wakabayashi, Y. Krockenberger, T. Nomura, Y. Kohama, S. A. Nikolaev, H. Das, H. Irie,

- K. Takiguchi, S. Ohya, M. Tanaka, Y. Taniyasu, and H. Yamamoto, npj Quantum Mater. 7, 102 (2022).
- [38] S. Kaneta-Takada, Y. K. Wakabayashi, Y. Krockenberger, H. Irie, S. Ohya, M. Tanaka, Y. Taniyasu, and H. Yamamoto, Phys. Rev. Mater. 7, 054406 (2023).
- [39] U. Kar, A. Kr. Singh, Y.-T. Hsu, C.-Y. Lin, B. Das, C.-T. Cheng, M. Berben, S. Yang, C.-Y. Lin, C.-H. Hsu, S. Wiedmann, and W.-C. Lee, and W.-L. Lee, npj Quantum Mater. 8, 8 (2023).
- [40] S. Itoh, Y. Endoh, T. Yokoo, S. Ibuka, J.-G. Park, Y. Kaneko, K. S. Takahashi, Y. Tokura, and Naoto Nagaosa, Nat. Commun. 7, 11788 (2016).
- [41] W. Lin et al., Adv. Mater. 33, 2101316 (2021).
- [42] A. J. Grutter, F. J. Wong, E. Arenholz, A. Vailionis, and Y. Suzuki, Phys. Rev. B 85, 134429 (2012).
- [43] D. D. Sarma, P. Sen, C. Carbone, R. Cimino, and W. Gudat, Phys. Rev. B 39, 12387 (1989).
- [44] Y. Ishida, R. Eguchi, M. Matsunami, K. Horiba, M. Taguchi, A. Chainani, Y. Senba, H. Ohashi, H. Ohta, and S. Shin, Phys. Rev. Lett. 100, 056401 (2008).
- [45] D. H. Kim, E. Lee, H. W. Kim, S. Kolesnik, B. Dabrowski, C.-J. Kang, M. Kim, B. I. Min, H.-K. Lee, J.-Y. Kim, and J.-S. Kang, Phys. Rev. B 91, 075113 (2015).
- [46] S. Carlotto, M. M. Natile, A. Glisenti, and A. Vittadini, Chem. Phys. Lett. 588, 102 (2013).
- [47] S. Kaneta-Takada, Y. K. Wakabayashi, Y. Krockenberger, S. Ohya, M. Tanaka, Y. Taniyasu, and H. Yamamoto, Appl. Phys. Lett. 118, 092408 (2021).
- [48] See Supplemental Material at http://link.aps.org/supplemental/10.1103/n9qh-6739 for Sec. I crystal structure of $SrRuO_3/SrTiO_3$ thin films, Sec. II core-level X-ray photoemission spectroscopy spectra, Sec. III procedure for subtracting the second order light contribution, Sec. IV negligible contribution of surface contamination, and Sec. V how to estimate U_{pp} by the Cini-Sawatzky method.
- [49] K. Ishigami, K. Yoshimatsu, D. Toyota, M. Takizawa, T. Yoshida, G. Shibata, T. Harano, Y. Takahashi, T. Kadono, V. K. Verma, V. R. Singh, Y. Takeda, T. Okane, Y. Saitoh, H. Yamagami, T. Koide, M. Oshima, H. Kumigashira, and A. Fujimori, Phys. Rev. B 92, 064402 (2015).
- [50] D. E. Shai, C. Adamo, D. W. Shen, C. M. Brooks, J. W. Harter, E. J. Monkman, B. Burganov, D. G. Schlom, and K. M. Shen, Phys. Rev. Lett. 110, 087004 (2013).

- [51] K. Fujioka, J. Okamoto, T. Mizokawa, A. Fujimori, I. Hase, M. Abbate, H. J. Lin, C. T. Chen, Y. Takeda, and M. Takano, Phys. Rev. B 56, 6380 (1997).
- [52] E. B. Guedes, M. Abbate, K. Ishigami, A. Fujimori, K. Yoshimatsu, H. Kumigashira, M. Oshima, F. C. Vicentin, P. T. Fonseca, and R. J. O. Mossanek, Phys. Rev. B 86, 235127 (2012).
- [53] H. Jeong, S. G. Jeong, A. Y. Mohamed, M. Lee, W.-S. Noh, Y. Kim, J.-S. Bae, W. S. Choi, and D.-Y. Cho, Appl. Phys. Lett. 115, 092906 (2019).
- [54] J. Kim, J. Chung, and S.-J. Oh, Phys. Rev. B **71**, 121406(R) (2005).
- [55] J. Okamoto, T. Okane, Y. Saitoh, K. Terai, S.-I. Fujimori, Y. Muramatsu, K. Yoshii, K. Mamiya, T. Koide, A. Fujimori, Z. Fang, Y. Takeda, and M. Takano, Phys. Rev. B 76, 184441 (2007).
- [56] M. Takizawa, D. Toyota, H. Wadati, A. Chikamatsu, H. Kumigashira, A. Fujimori, M. Oshima, Z. Fang, M. Lippmaa, M. Kawasaki, and H. Koinuma, Phys. Rev. B 72, 060404(R) (2005).
- [57] L. H. Tjeng, C. T. Chen, and S-W. Cheong, Phys. Rev. B 45, 8205 (1992).
- [58] L. C. Davis and L. A. Feldkamp, Phys. Rev. B 23, 6239 (1981).
- [59] S. Hüfner, Photoemission Spectroscopy (Springer, Berlin, Heidelberg, 2003).
- [60] O. Tjernberg, S. Söderholm, U. O. Karlsson, G. Chiaia, M. Qvarford, H. Nylén, and I. Lindau, Phys. Rev. B 53, 10372 (1996).
- [61] Y. Tezuka, S. Shin, T. Uozumi, and A. Kotani, J. Phys. Soc. Jpn. 66, 3153 (1997).
- [62] L. C. Davis and L. A. Feldkamp, J. Appl. Phys. 50, 1944 (1979).
- [63] Z. V. Pchelkina, I. A. Nekrasov, T. Pruschke, A. Sekiyama, S. Suga, V. I. Anisimov, and D. Vollhardt, Phys. Rev. B 75, 035122 (2007).
- [64] J. Mravlje, M. Aichhorn, T. Miyake, K. Haule, G. Kotliar, and A. Georges, Phys. Rev. Lett. 106, 096401 (2011).
- [65] U. D. Wdowik and K. Parlinski, Phys. Rev. B 75, 104306 (2007).
- [66] J. G. Bednorz and K. A. Müller, Z. Phys. B 64, 189 (1986).
- [67] C. Weber, C. Yee, K. Haule, and G. Kotliar, Europhys. Lett. 100, 37001 (2012).